Journal of Medicinal Chemistry

Article

Cite This: J. Med. Chem. 2019, 62, 1291−1305

pubs.acs.org/jmc

Antiproliferative and Antimigratory Effects of a Novel YAP−TEAD Interaction Inhibitor Identified Using in Silico Molecular Docking

Sarah A. Smith,[†] Richard B. Sessions,[‡] Deborah K. Shoemark,[‡] Christopher Williams,[§] Reza Ebrahimighaei,[†] Madeleine C. McNeill,[†] Matthew P. Crump,[§] Tristan R. McKay,[∥] Gemma Harris,[⊥] Andrew C. Newby,[†] and Mark Bond*[,†]

[†]School of Translational Health Sciences, Faculty of Health Sciences, University of Bristol, Research Floor Level 7, Bristol Royal Infirmary, Bristol BS2 8HW, U.K.

[‡]School of Biochemistry, Faculty of Biomedical Sciences, University of Bristol, Biomedical Sciences Building, University Walk, Bristol BS8 1TD, U.K.

[§]School of Chemistry, Faculty of Science, University of Bristol, Cantock's Close, Bristol BS8 1TS, U.K.

[∥]Centre for Bioscience, Manchester Metropolitan University, John Dalton Building, Manchester M1 5GD, U.K.

[⊥]Research Complex at Harwell, Rutherford Appleton Laboratory, Harwell Campus, Didcot, Oxfordshire OX11 0FA, U.K.

Supporting Information

ABSTRACT: The Hippo pathway is an important regulator of cell growth, proliferation, and migration. TEAD transcription factors, which lie at the core of the Hippo pathway, are essential for regulation of organ growth and wound repair. Dysregulation of TEAD and its regulatory cofactor Yes-associated protein (YAP) have been implicated in numerous human cancers and hyperproliferative pathological processes. Hence, the YAP−TEAD complex is a promising therapeutic target. Here, we use in silico molecular docking using Bristol University Docking Engine to screen a library of more than 8 million druglike molecules for novel disrupters of the YAP−TEAD interaction. We report the identification of a novel compound (CPD3.1) with the ability to disrupt YAP−TEAD protein−protein interaction and inhibit TEAD activity, cell proliferation, and cell migration. The YAP−TEAD complex is a viable drug target, and CPD3.1 is a lead compound for the development of more potent TEAD inhibitors for treating cancer and other hyperproliferative pathologies.

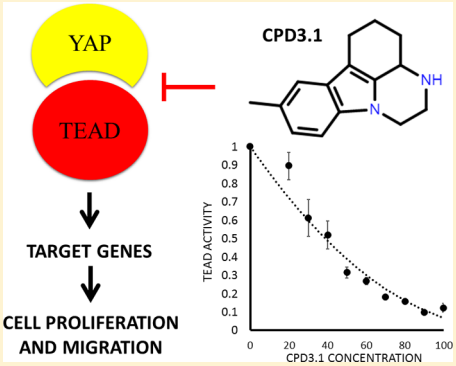

INTRODUCTION

The oncogenic Hippo signaling pathway has emerged as an important regulator of cell growth,[1] proliferation,[2] and migration.[3] TEAD transcription factors (TEAD1−4), at the core of the Hippo pathway, are essential for regulation of normal organ size, cardiogenesis,[4] formation of the trophectoderm[5] in embryos, and wound repair in adults.[3] Dysregulation of TEAD proteins has been implicated in numerous human cancers, including breast cancers,[6] fallopian tube carcinoma,[7] germ cell tumors,[8] renal cell carcinoma,[9] medulloblastoma,[10] and gastric cancer.[11] Increased TEAD activity can induce oncogenic transformation.[12−14] Moreover, increased TEAD protein expression in gastric,[15] colorectal,[16] breast,[6] and prostate cancers[17] is associated with reduced patient survival. Dysregulated TEAD activity has also been associated with other hyperproliferative pathological processes, including angioplasty restenosis.[18]

Transcriptional activation by TEAD is dependent on interaction with transcriptional cofactors. The best characterized TEAD cofactors are Yes-associated protein (YAP) and transcriptional coactivator with PDZ-binding motif (TAZ).[19] However, other proteins have also been reported to have TEAD cofactor activity, including members of the Vgll family[20−22] and p160 family of nuclear receptor cofactors.[23] The activity of YAP and TAZ is negatively regulated by the Hippo pathway kinase LATS1,[24−27] which can occur in response to actin cytoskeleton disruption. Phosphorylation of YAP and TAZ triggers their nuclear export and proteasomal degradation. Although YAP and TAZ appear to be dispensable for normal homeostasis of many adult organs,[28] they play essential roles promoting tissue repair following injury.[29,30] As with the TEAD proteins, YAP and TAZ activation has been identified in many human tumors and is essential for tumor initiation, progression, and metastasis.[31] Furthermore, elevated expression of YAP is associated with reduced survival in patients with breast,[32] ovarian,[33] colon,[34] liver,[35] and pancreatic[36] cancers. Consistent with this, the activation or overexpression of YAP or TAZ enhances TEAD-dependent gene expression (e.g., *CCN1*, *CTGF*, *ITGB2*, and Birc5/Survivin) and promotes cell proliferation and migration in many cell types.[37] Conversely, signals or interventions that

Received: September 10, 2018
Published: January 14, 2019

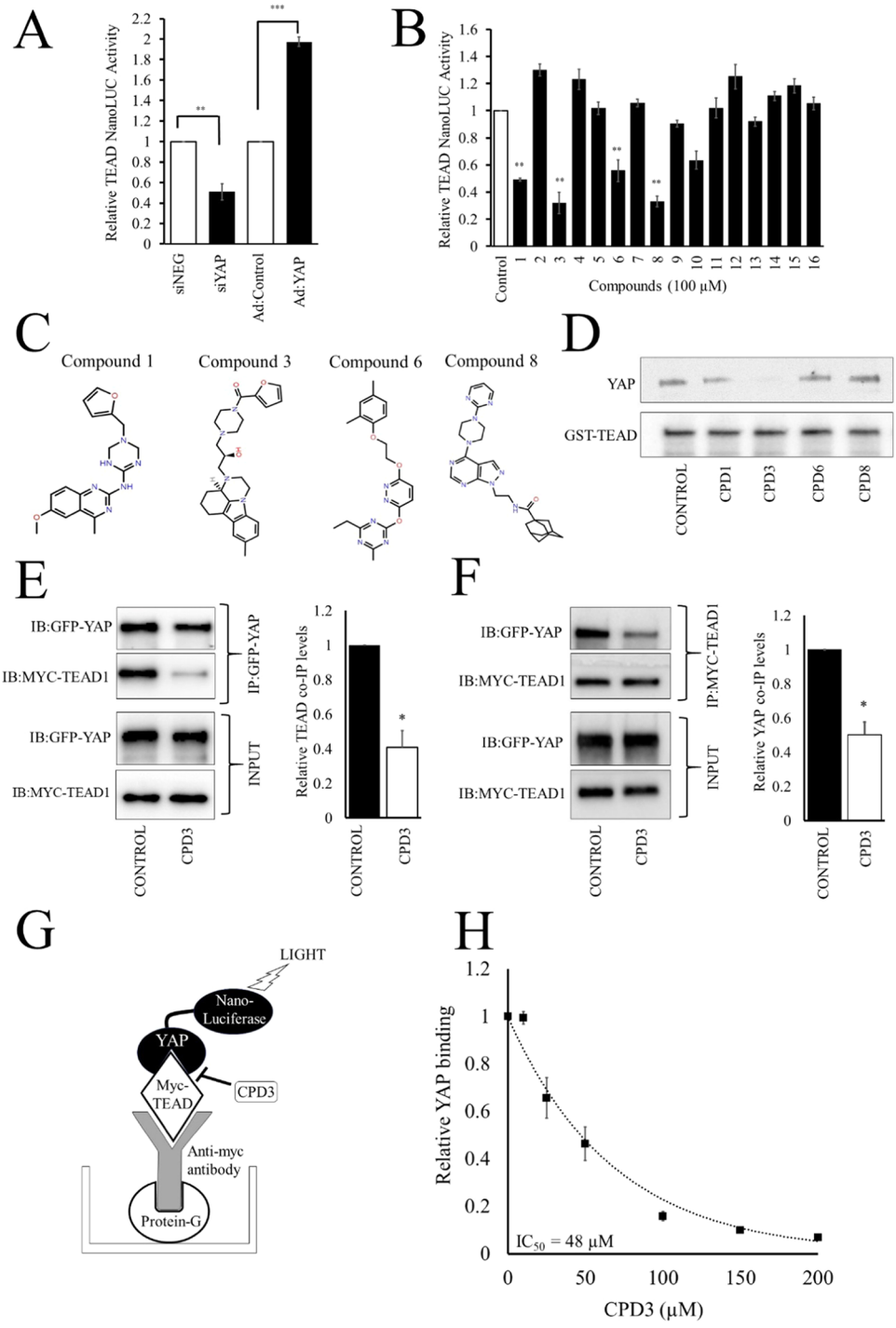

Figure 1. BUDE screening-identified compound 3 for TEAD inhibition. (A) HeLa cells were stably transduced with a lentiviral viral vector containing 8×TEAD-secreted nanoluciferase reporter gene (TEAD-NLUC). Cells were transfected with non-targeting siRNA (siNEG), siRNA targeting YAP (siYAP), control adenoviral vector or an adenovirus expression constitutively active $YAP5S_{127A}$ (Ad:YAP). Culture media were conditioned for 6 h and assayed for secreted nanoluciferase activity ($n = 3$). (B) HeLa cells stably transduced with TEAD-NLUC were treated with 100 μM of indicated compound for 6 h. Cell conditioned media were assayed for nanoluciferase activity ($n = 3$). (C) Chemical structure of compounds that statistically significantly inhibited TEAD-NLUC activity. (D) Recombinant GST-TEAD1 protein bound to glutathione resin was incubated with 200 μM of the indicated compounds and HEK293 cell lysate containing endogenous YAP protein for 18 h at 4 °C. The resin was washed, and bound YAP eluted and quantified by Western blotting ($n = 2$). (E and F) HeLa cells were transfected with myc-TEAD1 or GFP-YAP plasmids and total cell lysates prepared. Myc-TEAD lysates incubated with 200 μM of CPD3 for 3 h before addition of GFP-YAP lysate. Myc-TEAD:GFP-YAP complexes were co-immunoprecipitated with either GFP-Trap (E; $n = 3$) or myc-TRAP (F; $n = 3$). Co-immunoprecipitated YAP or TEAD was quantified by Western blotting. Schematic illustration of 96 well plate YAP-TEAD interaction assay (G). Dose response analysis of disruption YAP-NL interaction with myc-TEAD by CPD3.1 (H). * = $p < 0.05$, ** = $p < 0.01$, *** = $p < 0.001$.

block the formation of YAP/TAZ−TEAD complexes prevent the expression of many mitogenic TEAD target genes and dramatically reduce cell proliferation and oncogenic transforming activity.[37−40]

DOI: 10.1021/acs.jmedchem.8b01402
J. Med. Chem. 2019, 62, 1291−1305

Multiple and diverse signals induce nuclear translocation of YAP and TAZ, including cellular density GPCR ligands,[41] mitogens,[42] Wnts,[43] and extracellular matrix stiffness.[44] Conversely, multiple antimitogenic signals induce nuclear exclusion of YAP and TAZ and inhibition of TEAD-dependent gene expression.[39,45] This suggests that the YAP/TAZ−TEAD complex acts as a central point of convergence for multiple biochemical and mechanical signaling pathways that control cell proliferation and migration. Hence, there is considerable interest in targeting these proteins therapeutically, for example, for the treatment of cancer,[46] cardiovascular disease,[39] and liver fibrosis.[47] Targeting the Hippo pathway would be distinct from conventional cytotoxic chemotherapy or medications that lower low-density lipoprotein cholesterol, the current mainstays of cancer and cardiovascular disease treatment that, nevertheless, do not fully normalize risk. These multifactorial pathologies are characterized by dysregulation of multiple diverse signaling pathways that converge at a relatively small number of transcription factors, suggesting that targeting transcription factors may represent a highly promising, widely applicable therapeutic strategy. However, pharmacological targeting of transcription factors is challenging. Unlike enzymes, they often lack deep binding pockets for small molecules and instead rely on complex protein−protein interactions based on large surface areas, which are traditionally believed to be more difficult to target.[48]

Small molecules with YAP−TEAD inhibitory properties have been reported. For example, the TEAD inhibitory activity of the porphyrin molecule, verteporfin, was identified by screening a library of 3300 Food and Drug Administration-approved drugs.[14,40] Verteporfin inhibits YAP, at least in part, by stimulating levels of 14-3-3ε, which sequesters YAP in the cytoplasm.[40] Moreover, verteporfin is pleiotropic, having antiproliferative and cytotoxic effects independent of its effect on YAP.[27,49] Oku et al.[50] identified dasatinib, fluvastatin, and pazopanib as inhibitors of YAP/TAZ nuclear localization using image-based screening of 400 small molecules. Their mechanisms of action are unclear but may be mediated via inhibition of RhoA and disruption of actin polymerization.[50]

The recent elucidation of the crystal structure of the YAP−TEAD1 complex[51] (PDB accession code 3KYS) opens the possibility of rationally designed direct YAP−TEAD interaction inhibitors. Crystallography indicates that YAP protein wraps around the YAP-binding domain of TEAD1, forming extensive interactions over three distinct interaction interfaces. Structural and mutational studies identified a small number of highly conserved amino acids, namely, Ser_{94}, Phe_{95}, and Phe_{96}, located in the Ω-loop of YAP, part of interaction interface three, which are essential for YAP interaction with TEAD.[51] The side chains of these residues fit into a deep hydrophobic pocket on TEAD that has an excellent druggability score,[52,53] suggesting that the YAP−TEAD interaction may be a feasible drug target. Consistent with this, two groups have reported the design of peptides based on the YAP interaction interface with the ability to disrupt YAP−TEAD interaction,[54] albeit in a cell-free system. Use of peptide-based interaction inhibitors is limited by their poor cell permeability, with inhibition of TEAD activity only achieved via plasmid-based expression of FLAG-tagged peptide fusion proteins. Thermal-shift-assay-based screening of a small molecule fragment library has identified cell permeable small molecules that bind the TEAD hydrophobic pocket occupied by YAP Phe_{95}, but these molecules exhibited low potency, modestly inhibiting TEAD activity at millimolar concentrations.[55]

Here, we use in silico molecular docking using Bristol University Docking Engine (BUDE)[56,57] to screen more than 8 million clean (compounds with only benign functional groups[58]) and druglike molecules from the Zinc Is Not Commercial (ZINC) available compounds database for novel disrupters of the YAP−TEAD interaction. In contrast to most other docking algorithms, BUDE utilizes an empirical free-energy force field and is unique in using an atom−atom force field, which takes into account Wolfenden solvation energies. This allows BUDE to more accurately estimate the entropic cost/enthalpic gain encountered by a ligand, leaving a fully solvated state to bind to a protein. This is particularly important for interrogating the more challenging, flatter protein−protein or protein−ligand interactions because these often rely more heavily on hydrophobic interactions. Here, we describe a BUDE screening strategy that identified a shortlist of putative TEAD1-binding compounds, from which we characterize a novel compound that disrupts TEAD-dependent transcription, cell proliferation, and cell migration.

RESULTS

Identification of TEAD Inhibitors Using BUDE Molecular Docking. The enrichment process from the first BUDE docking reduced the number of conformers from 160 million to 100 000. The second BUDE run docked the 100 000 compounds into five structures extracted from the molecular dynamics (MD) simulation of TEAD1 (to represent the "breathing" motion of the unbound protein in solution and allowed for both side-chain and backbone flexibilities), which allowed the selection of 1000 compounds showing binding to at least four TEAD1 protein conformations (Supplement Figures 1 and 2). The selection process from 1000 (see Supplement Data File S1) to the final list of 16 compounds (Supplement Tables 1 and 3) for testing in vitro used the following set of criteria: (i) visual inspection to identify compounds that interacted with YAP binding pocket that accommodates the epsilon two carbon atom of the YAP Phe_{95} residue (Supplement Figure 1); (ii) maximizing the chemical diversity of the initial test set; (iii) favorable calculated (c Log P) or experimental (log P) solubility; and (iv) actual compound availability for purchase at a reasonable (<£200) cost per screening sample.

The shortlisted sets of 16 compounds were first assayed for their ability to inhibit TEAD-dependent transcriptional activity in HeLa cells that had been transduced with a recombinant lentiviral vector expressing secreted bioluminescent nanoluciferase (NLUC) reporter gene enzyme, which is expressed under the control of a promoter region containing eight TEAD DNA-binding elements (TEAD-NLUC). The reporter cell line was validated by showing that the expression of secreted nanoluciferase (NLUC) enzyme activity was significantly inhibited by siRNA-mediated silencing of the TEAD cofactor YAP (Figure 1A). Furthermore, the expression of secreted nanoluciferase (NLUC) enzyme activity was significantly stimulated by YAP overexpression (Figure 1A). These data demonstrate that this cell line faithfully reports YAP-dependent TEAD activity. Four of the compounds shortlisted (CPD1, 3, 6, and 8) significantly (>60%) inhibited TEAD-NLUC activity (Figure 1B,C), without significantly affecting cell viability (Supplement Figure 3), indicating that these compounds inhibited TEAD-dependent transcriptional activity.

DOI: 10.1021/acs.jmedchem.8b01402
J. Med. Chem. 2019, 62, 1291−1305

We next tested the ability of these four compounds to inhibit the binding of endogenous YAP protein present in HEK293 whole cell lysate to recombinant glutathione S-transferase (GST)−TEAD1 protein immobilized on glutathione resin beads. Western blotting of proteins binding the beads demonstrated that only CPD3 was able to inhibit the binding of YAP protein to GST−TEAD1 (Figure 1D). Inhibition of YAP binding to TEAD1 in the presence of CPD3 was further confirmed using co-immunoprecipitation assays using mammalian cell lysates prepared from HeLa expressing myc-TEAD1 and GFP−YAP. CPD3 inhibited binding of myc-TEAD1 to affinity-purified GFP−YAP (Figure 1E). Likewise, CPD3 also inhibited binding of GFP−YAP to immunoprecipitated myc-TEAD1 (Figure 1F). We next set up a 96-well plate-based YAP−TEAD interaction assay to determine the IC_{50} of the inhibition of the YAP−TEAD complex by CPD3. Myc-tagged-TEAD1 protein was immobilized on protein-G-coated plates using an anti-myc antibody and the interaction of a YAP−nanoluciferase fusion protein quantified in the presence of increasing concentrations of CPD3 (Figure 1G). Incubation with CPD3 resulted in a dose-dependent inhibition of YAP−nanoluciferase activity bound to the myc-TEAD1 protein-coated wells, indicating that CPD3 inhibited YAP interaction with TEAD1. The IC_{50} of the inhibition was calculated at 48 μM (Figure 1H).

The BUDE docking pose of CPD3 (Figure 2A,B; see PDB Data File) predicts that the planar indole-based aromatic ring

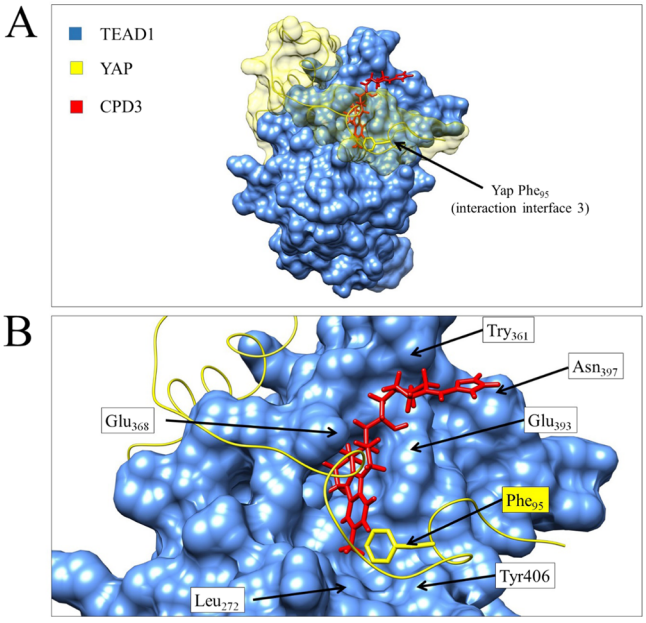

Figure 2. BUDE docking pose for compound 3. (A) Surface plot of TEAD1 (PDB:3kys) in blue with the YAP chain shown in yellow (with a transparent surface render) and compound 3 structure (red) binding pose. (B) Close up render of the TEAD1 hydrophobic pocket showing the compound 3 binding pose. The YAP Phe_{95} side-chain is depicted in yellow.

structure of CPD3 occupies the hydrophobic TEAD1 pocket bordered by residues Leu_{272}, Glu_{368}, Glu_{393}, and Try_{406} (residue numbering according to Li et al.[51]) in a vertical orientation. The docking pose predicts that CPD3 binds in a position close to the YAP Met_{86}, Ile_{91}, and Phe_{95} side chains (numbering according to sequence NP_068780). These hydrophobic side chains of YAP form multiple van der Waals contacts with I_{247}, V_{242}, L_{272}, V_{391}, and Y_{406} of TEAD1 (numbering according to Li et al.[51]) and are known to be essential for YAP binding.[51] The furyl moiety at the opposite end of the molecule occupies a cleft formed by TEAD1 Tyr_{376} and Asn_{411}.

Compound 3 Inhibits TEAD-Dependent Target Gene Expression, Cell Proliferation, and Migration. Activation of TEAD transcription factors in response to YAP binding induces the expression of many genes that encode proteins known to be involved in promoting cell proliferation and migration (see Supplement Figure 14). The best characterized TEAD target genes associated with the promotion of cell proliferation and migration are *CCN1* and *CTGF*.[39,59,60] For example, we have recently demonstrated such a role for YAP−TEAD-dependent regulation of *CCN1* in the regulation of vascular smooth muscle cell (VSMC) proliferation and migration.[39] We therefore tested whether CPD3 inhibited the promoter activity of known TEAD target genes, *CCN1* and *CTGF*, in the HeLa transformed cell line and primary rat VSMCs (RaVSMCs). Cells were transfected with plasmids expressing bioluminescent firefly luciferase reporter genes under the control of either the *CCN1* or *CTGF* promoter regions. Incubation with CPD3 for 6 h resulted in a strong and significant dose-dependent inhibition of *CCN1*- and *CTGF*-luciferase reporter gene activities in both HeLa cells (Figure 3A) and RaVSMCs (Figure 3B). As both *CCN1* and *CTGF* are classical TEAD target genes, this is consistent with the inhibition of TEAD activity by CPD3. Importantly, activity of the TEAD-independent minimal *TNT1* gene promoter, which lacks TEAD-binding elements, was not inhibited by any concentration of CPD3 tested, indicating that CPD3 selectively inhibits TEAD-dependent transcription and does not nonspecifically reduce the transcription of TEAD-independent genes. Furthermore, steady-state mRNA levels of endogenous *CCN1* and *CTGF* genes, which are known to be involved in the promotion of cell proliferation and migration, but not the TEAD-independent housekeeping gene *36B4*, were also significantly inhibited by CPD3 (Supplement Figure 4). CPD3 also dose-dependently inhibited cell proliferation (detected by the incorporation of EdU into newly synthesized DNA (Figure 3C,D)) and migration (detected by real-time scratch wound assay), in both HeLa (Figure 3E) and RaVSMCs (Figure 3F and Supplement Figure 5).

Functional Analysis of Compound 3 Fragments. We tested three small molecular fragments of CPD3 for TEAD inhibitory activity. CPD3.1 represents the planar aromatic ring structure of CPD3, CPD3.2 is a piperazinyl propanediol representing the mid-region of CPD3, and CPD3.3 represents the terminal furyl group (Figure 4A). Dose−response analysis demonstrated that CPD3 significantly inhibited TEAD-dependent NLUC secretion in HeLa at 60 μM with IC_{50} > 110 μM (Figure 4B) but did not affect cell viability (Supplement Figure 6) or have any direct inhibitory effect on NLUC enzymatic activity at any concentration tested (Supplement Figure 7A). CPD3.1 also significantly inhibited TEAD-dependent NLUC secretion at 20 μM with IC_{50} = 70 μM (Figure 4C), without affecting cell viability (Supplement Figure 6) and without having any direct inhibitory effect on NLUC activity (Supplement Figure 7B). Although not strictly applicable to this type of indirect reporter gene assay, the Hill slopes for both CPD3 and CPD3.1 (Figure 4B,C) were close to 1 (0.77 and 0.73, respectively). Although CPD3.1 appeared

DOI: 10.1021/acs.jmedchem.8b01402
J. Med. Chem. 2019, 62, 1291−1305

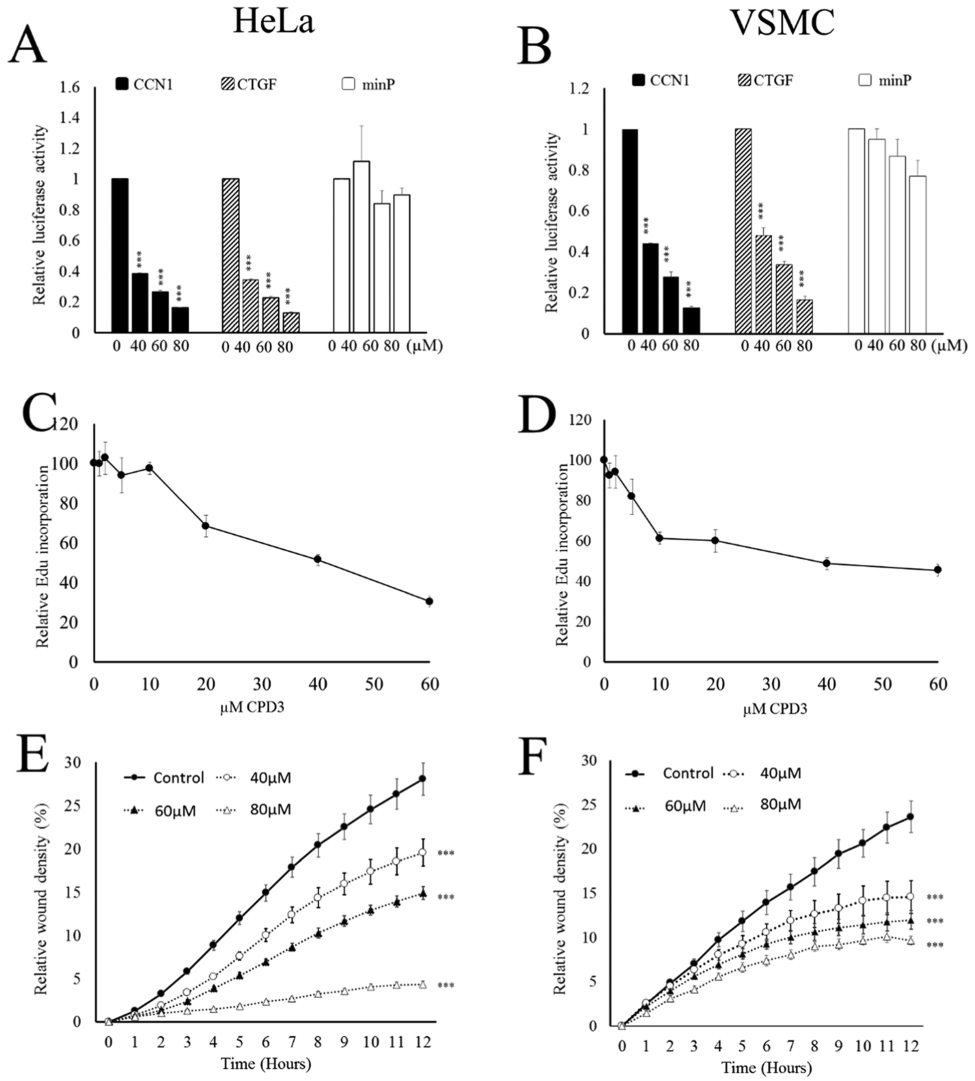

Figure 3. Compound 3 inhibits TEAD target gene expression, cell proliferation, and cell migration. HeLa cells (A) and RaVSMCs (B) were transfected with *CCN1*-LUC, *CTGF*-LUC or minimal promoter-LUC (minP-LUC) reporter plasmids and treated with indicated concentrations of compound 3 for 6 h. Cell lysates were assayed for fire-fly luciferase activity ($n = 3$). HeLa cells (C) and RaVSMCs (D) were treated with indicated concentrations of compound 3 for 18 h, followed by a 6 h labeling with 10 μM EdU ($n = 4$). HeLa cells (E) and RaVSMCs (F) were treated with the indicated concentrations of compound 3 and migration quantified using a real-time IncuCyte scratch wound assay ($n = 4$). * = $p < 0.05$, ** = $p < 0.01$, *** = $p < 0.001$.

to be a more potent inhibitor of TEAD activity in these cell-based assays, this may simply reflect increased cell permeability compared to CPD3. Neither CPD3.2 nor CPD3.3 had any effect on TEAD-NLUC activity (Figure 4D,E) or cell viability (Supplement Figure 6). This suggests that the planar indole-based aromatic ring structure of CPD3.1 represents the functional YAP−TEAD inhibitory group. BUDE docking of CPD3.1 (see PDB Data File) predicts that this compound occupies the TEAD pocket in a similar pose to CPD3 (root-mean-square deviation (RMSD) between corresponding atoms is 2.42 Å) (Figure 5A,B). Binding of CPD3.1 to purified recombinant TEAD protein was confirmed by saturation transfer difference (STD) NMR (Figure 6) and isothermal titration calorimetry (Supplement Figure 8), which estimated the binding affinity to TEAD1 in the low micromolar range (~12 μM).

TEAD proteins (TEAD1−4) display a high degree of sequence conservation in residues that create the hydrophobic pocket that is essential for YAP binding.[51] YAP proteins also display a high degree of conservation in residues that interact with this pocket.[51] We therefore tested whether CPD3.1 was able to inhibit YAP-induced activity of TEAD1, TEAD2, TEAD3, and TEAD4. To quantify the effect of CPD3.1 on the activity of each individual TEAD paralog, while excluding interference from endogenously expressed TEAD1−4 proteins, we expressed each TEAD paralog (TEAD1−4) fused to the yeast GAL4 DNA-binding domain. Cells were transfected with the GAL4−TEAD expression vector together with a secreted nanoluciferase reporter gene vector under control of a promoter containing five GAL4 DNA-binding elements. This system allows us to study the effect of CPD3.1 on the activity of each individual TEAD protein in isolation, without interference from endogenously expressed transcription factors. In addition, the cells were co-transfected with a YAP expression vector to activate the GAL4−TEAD fusion-dependent transcription (see Supplement Figure 9). Basal activities of TEAD1, TEAD2, TEAD3, and TEAD4 were inhibited by CPD3.1 (Figure 7A−D). This likely reflects the

DOI: 10.1021/acs.jmedchem.8b01402
J. Med. Chem. 2019, 62, 1291−1305

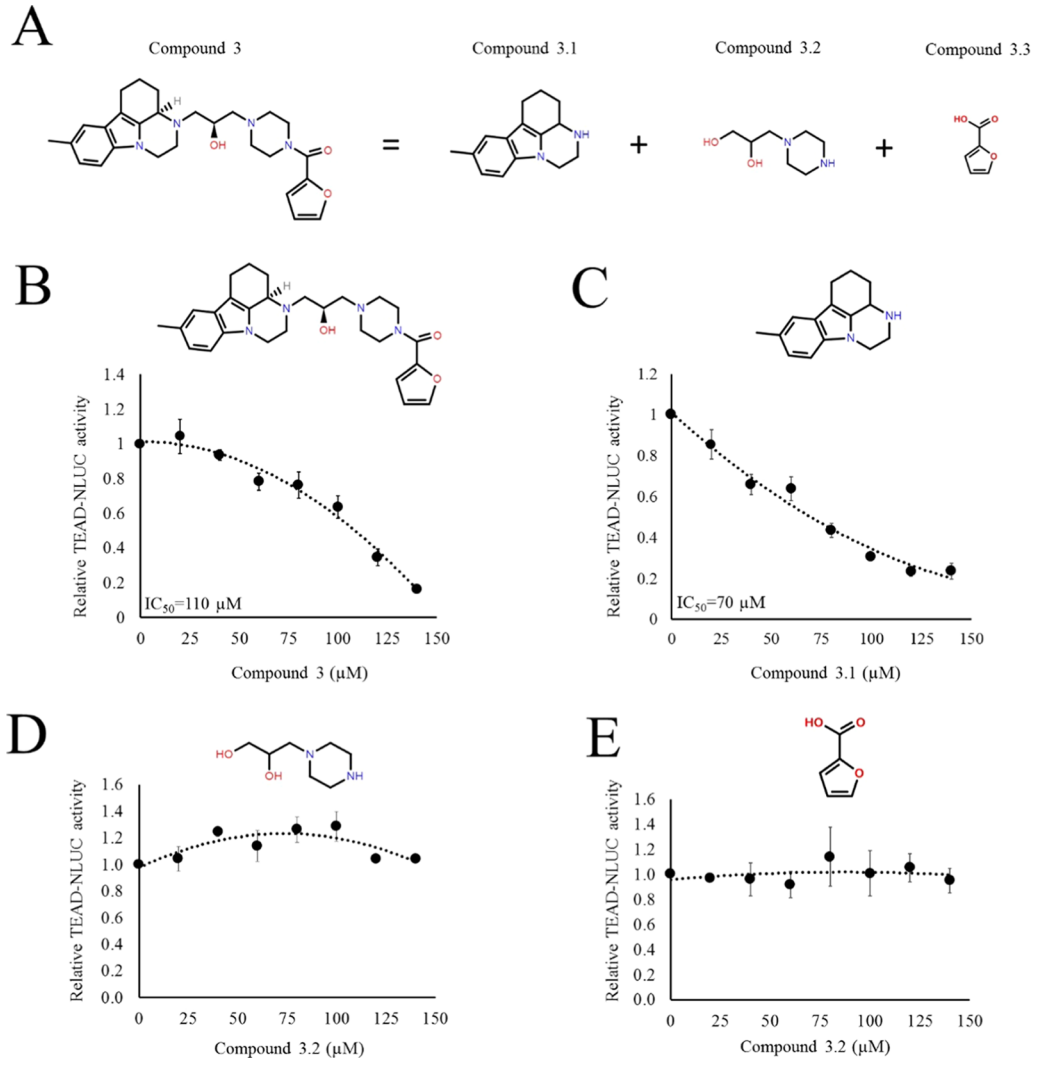

Figure 4. Functional analysis of compound 3 fragments. (A) Chemical structures of compound 3 and fragments of compound 3 (compound **3.1** − **3.3**). HeLa cells stably expressing TEAD-NLUC were treated with indicated concentrations of compound 3 (n = 3) (B), compound **3.1** (n = 3) (C), compound **3.2** (n = 3) (D), compound **3.3** (n = 3) (E) for 6 h. Secreted nano-luciferase activity was quantified in the cell conditioned media.

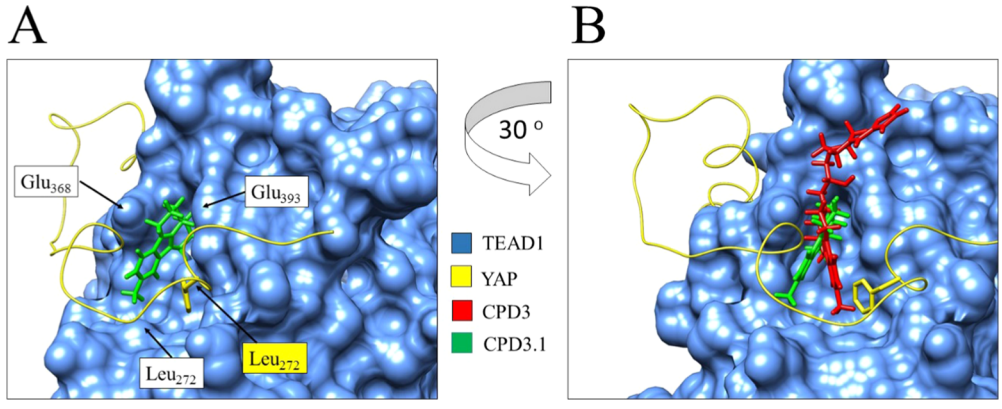

Figure 5. BUDE docking pose for compound 3.1. (A) Surface plot of TEAD1 (PDB:3kys) in blue with the YAP chain shown in yellow and compound 3.1 structure binding pose (green). (B) Close up render of the TEAD1 hydrophobic pocket showing the compound 3.1 (green) and compound 3 (red) binding pose. The YAP Phe_{95} side-chain is depicted in yellow.

inhibition of TEAD activity driven by endogenous expression of YAP. Activity of all four TEAD paralogs was stimulated by YAP overexpression and this was significantly inhibited by CPD3.1 (Figure 7A−D). This suggests that the conservation of residues forming the YAP binding TEAD pocket allows CPD3.1 to inhibit YAP activation of all TEAD paralogs. Dose−response analysis demonstrated that CPD3.1 inhibited YAP-induced TEAD1 activity with IC_{50} = 40 μM (Figure 7E),

DOI: 10.1021/acs.jmedchem.8b01402
J. Med. Chem. 2019, 62, 1291−1305

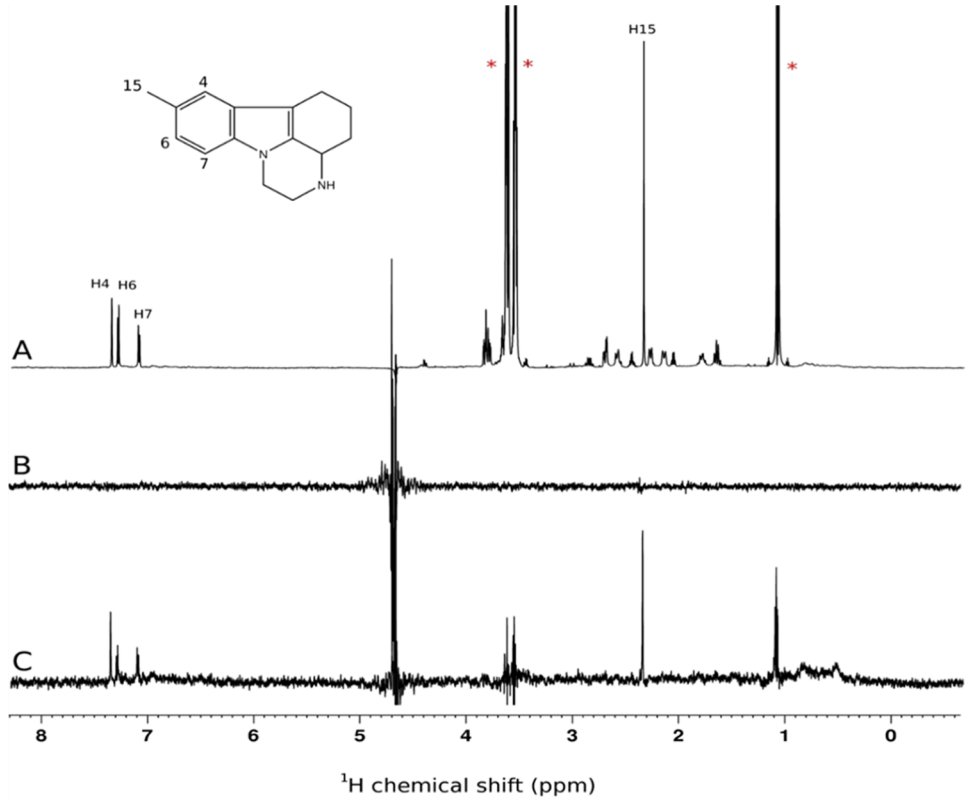

Figure 6. Saturation transfer difference (STD) NMR analysis of compound 3.1 binding to TEAD1. Saturation-Transfer Difference (STD) NMR spectra showing the binding of CPD3.1 to recombinant TEAD1. (A) reference 1H NMR spectra of a mixture of CPD3.1 and TEAD1. (B) and (C) show the STD spectra of CPD3.1 in the absence and presence of TEAD1. The asterisk indicates buffer components or impurities in the sample. The three spectra were recorded in PBS made up in 40% H_2O/60% D_2O acquired at 700 MHz. The concentration of CPD3.1 was 2 mM, whereas the final concentration of TEAD1 was approximately 20 μM.

TEAD2 activity with IC_{50} = 33 μM (Figure 7F), TEAD3 activity with IC_{50} = 44 μM (Figure 7G), and TEAD4 activity with IC_{50} = 36 μM (Figure 7H). Importantly, CPD3.1 did not inhibit the basal activity of a TEAD-independent GAL4 reporter vector (Supplement Figure 10A). As a negative control to test for any off-target effects of CPD3.1, we used a reporter gene vector for a different transcription factor. For this, we used a serum response factor (SRF) reporter gene containing five serum response factor-binding elements instead of TEAD-binding elements. The cells were co-transfected with the SRF reporter gene together with a plasmid expressing serum response factor (SRF) protein fused to the VP16 transcriptional activation domain of herpes simplex virus type I (SRF−VP16). Expression of the SRF−VP16 fusion protein strongly activates the SRF-dependent reporter gene, allowing us to detect any inhibition of SRF activity. The SRF-dependent reporter gene activity was not inhibited by CPD3.1, thus providing more evidence of its selectivity for TEAD (Supplement Figure 10B).

CPD3.1 Inhibits TEAD Target Gene Expression, Cell Proliferation, and Cell Migration. Since the smaller CPD3.1 fragment retains TEAD inhibitory activity, we next tested whether CPD3.1 was able to inhibit TEAD target gene expression, cell proliferation, and cell migration in HeLa and RaVSMCs. Incubation of HeLa cells with CPD3.1 resulted in a dose-dependent inhibition of *CCN1*- and *CTGF*-luciferase reporter gene activities without affecting expression from the TEAD-independent minimal *TNT1* promoter (Figure 8A), consistent with specific inhibition of TEAD activity. *CCN1* and *CTGF* genes have previously been implicated in the regulation of cell proliferation and migration.[39] Consistent with this, CPD3.1 also dose-dependently inhibited HeLa cell proliferation (Figure 8B), with EdU incorporation significantly inhibited at doses above 40 μM. CPD3.1 also significantly inhibited HeLa cell migration at 40, 60, and 80 μM (Figure 8C).

In RaVSMCs, CPD3.1 dose-dependently inhibited TEAD-NLUC activity (Figure 9A; IC_{50} = 24 μM) and *CCN1-LUC* (Figure 9B; EC_{50} = 48 μM) and *CTGF-LUC* (Figure 9C; EC_{50} = 58 μM) luciferase reporter gene activities. Moreover, the expression of steady-state mRNA levels for known TEAD target genes (*CCN1*, *CTGF*, *PAI1*, *THBS*, *MAYDM*, and *MYOC*) was also significantly inhibited by CPD3.1 (Figure 9D). Dose−response experiments demonstrated the inhibition of *THBS* at 10 μM, *CCN1* at 20 μM, and *CTGF* at 40 μM (Supplement Figure 11). However, steady-state mRNA levels of the TEAD-independent housekeeping genes *PGK1*, *TBP*, *GAPDH*, and *36B4* were unaffected (Figure 9E), indicating that CPD3.1 selectively inhibits TEAD-dependent target gene expression and not simply by globally inhibiting transcription. Western blotting of total cell lysates also demonstrated that CPD3.1 inhibited the expression of *CCN1* protein levels (Figure 9F), confirming that these inhibitory effects translate into a reduction in protein levels. Incubation of RaVSMC (Figure 9G) or human VSMC (Figure 9H) with CPD3.1 for 18 h resulted in a dose-dependent inhibition of cell proliferation, detected by EdU incorporation. The EC_{50} for the inhibition of proliferation was 10 μM in RaVSMC and 1.5

DOI: 10.1021/acs.jmedchem.8b01402
J. Med. Chem. 2019, 62, 1291−1305

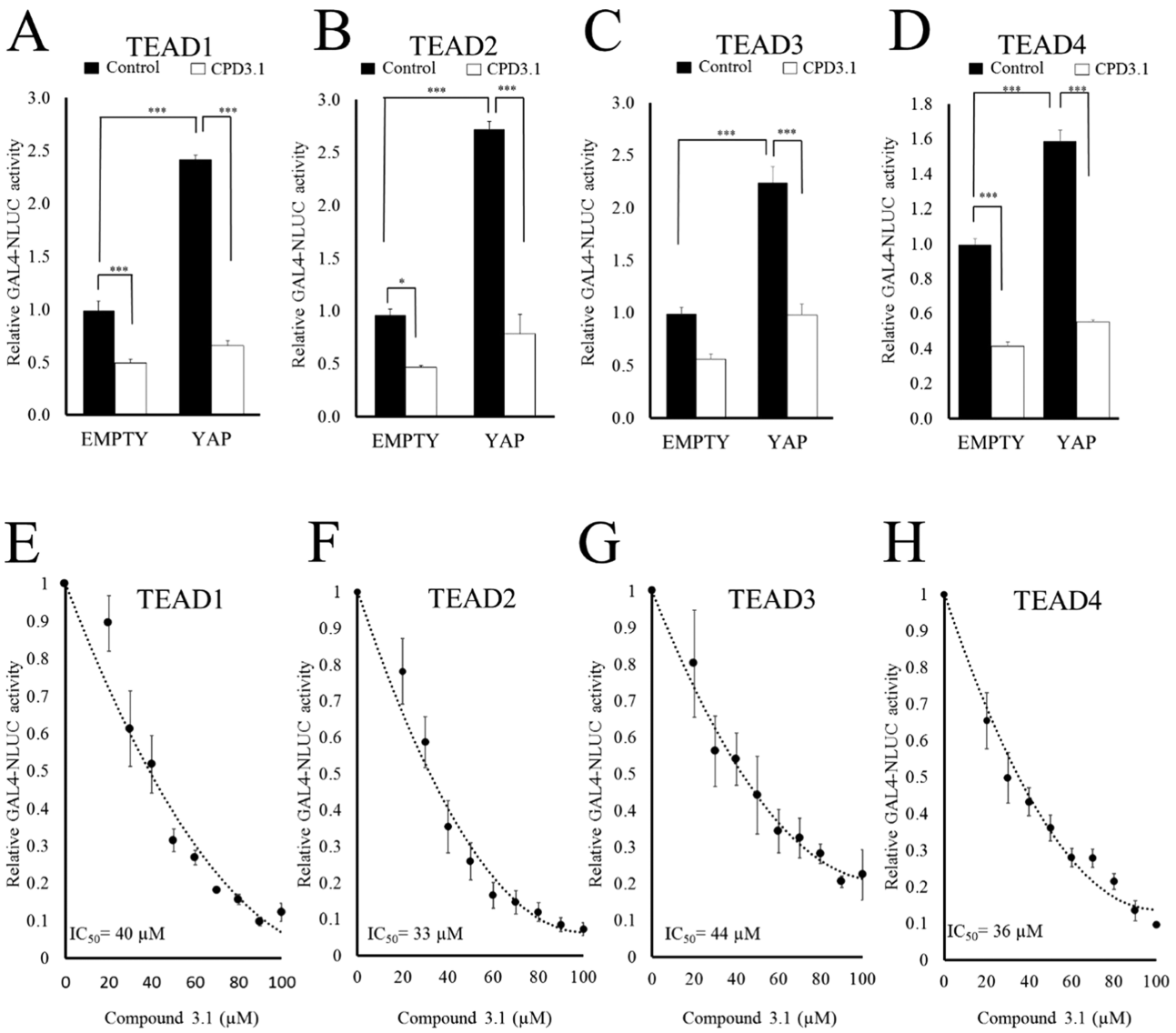

Figure 7. Compound 3.1 inhibits TEAD1, TEAD2, TEAD3, and TEAD4 activities. HeLa cells were transfected with a 5×GAL4-secNLUC reporter, together with expression vectors for GAL4-TEAD1, GAL4-TEAD2, GAL4-TEAD3 or GAL4-TEAD4 as indicated (A–H). In addition, cells were also transfected with plasmids expressing YAP (A–H) as indicated. EMPTY indicated a control plasmid lacking a transgene. Cells were treated with 100 μM (A–D) or indicated concentrations of compound 3.1 (E–H) and media were conditioned for 6 h. Secreted nano-luciferase activity was quantified in the conditioned media. (n = 3) * = p < 0.05, *** = p < 0.001.

μM in HuVSMC. RaVSMC and HuVSMC migration was similarly inhibited in a dose-dependent manner by 2, 10, and 20 μM CPD3.1 in RaVSMC (Figure 9I) and 0.25, 0.5, 2, and 10 μM in HuVSMC (Figure 9J). Importantly, CPD3.1 did not inhibit the proliferation of MCF7 cells (Supplement Figure 12), which have previously been reported to exhibit YAP–TEAD-independent growth.[50]

■ DISCUSSION AND CONCLUSIONS

Here, we report the discovery of a novel low-molecular-weight YAP–TEAD protein–protein interaction inhibitor using an in silico molecular docking screen of over 8 million druglike compounds. We report that CPD3 blocks YAP interaction with TEAD1 and inhibits TEAD activity, TEAD target gene expression, cell proliferation, and cell migration. Analysis of smaller fragment of CPD3 identified CPD3.1, which retains TEAD inhibitory activity. This compound displays more potent TEAD inhibitory activity in live cell assays, although this may be due, at least in part, to improved cell permeability. This study demonstrates that in silico molecular docking using the BUDE algorithm is a fast and cost-effective method for screening very large numbers of druglike small molecules to identify novel protein–protein interaction inhibitors. More importantly, it demonstrates that the TEAD pocket, which is responsible for YAP binding, is a viable drug target. The molecules we describe are likely to represent valuable lead compounds for the future development of potent TEAD inhibitors.

Until recently, the computational cost, in terms of hardware, time, and electricity consumption, of performing in silico molecular docking to screen libraries of millions of compounds was prohibitive. However, recent advances in modern computer processing power mean that this approach is now viable for augmenting or even replacing traditional screening methods. Utilizing multiple graphics processing units in the University of Bristol's BlueCrystal supercomputer, we com-

DOI: 10.1021/acs.jmedchem.8b01402
J. Med. Chem. 2019, 62, 1291–1305

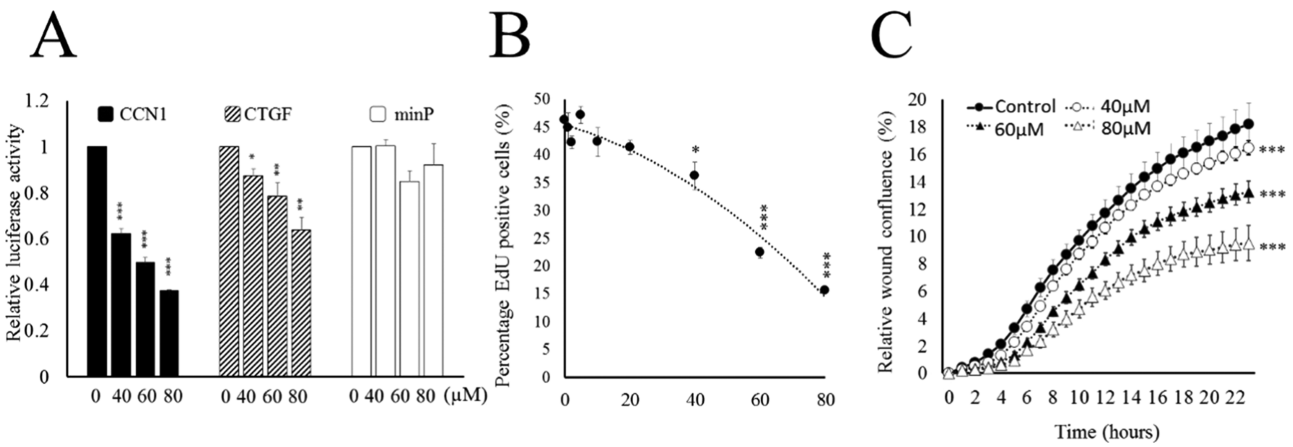

Figure 8. Compound 3.1 inhibits TEAD target gene expression, cell proliferation, and cell migration in HeLa cells. (A) HeLa cells were transfected with *CCN1*-FUC, *CTGF*-LUC or minimal promoter-LUC (minP-LUC) reporter plasmids and treated with indicated concentrations of compound 3.1 for 6 hr. Cell lysates were assayed for fire-fly luciferase activity (n = 3). (B) HeLa were treated with indicated concentrations of compound 3.1 for 18 h, followed by 6 h labeling with 10 μM EdU (n = 4). HeLa cells were treated with the indicated concentrations of compound 3.1 and migration quantified using a real time IncuCyte scratch wound assay (n = 4). * = $p < 0.05$, *** = $p < 0.001$.

pleted the initial screen of 8 million compounds within a few weeks. Subsequent validation of the short-listed compounds identified four compounds with TEAD inhibitory activity, demonstrating the efficacy of the BUDE algorithm. We focused our attention on CPD3 because this compound inhibited TEAD activity and disrupted YAP interaction. However, other compounds identified by our screen were able to inhibit TEAD activity without detectable effects on YAP interaction, suggesting that the occupation of the TEAD pocket by small molecules may be able to disrupt TEAD function, even when YAP remains bound. A similar disruption of TEAD function has been proposed to explain the TEAD inhibitory activity of flufenamates.[52] It is possible that these compounds induce subtle conformational changes in the YAP−TEAD complex or block important posttranslational modifications that are important for TEAD function, such as palmitoylation.[52,61] The docking pose for CPD3 predicts that the large planar aromatic ring structure, present at one end of the molecule, occupies the TEAD pocket and occludes the hydrophobic side chains of YAP Met_{86}, Ile_{91}, and Phe_{95} previously demonstrated to be essential for YAP interaction.[51] Consistent with this, a fragment of CPD3, termed CPD3.1 that is based only on this aromatic ring structure, is predicted to bind the pocket in a similar position and retains TEAD inhibitory activity. In TEAD-dependent reporter gene assays, CPD3.1 was more potent than the parental compound CPD3 with IC_{50} = 70 μM compared to IC_{50} = 110 μM for CPD3. This may reflect increased cell permeability, increased compound stability, or increased affinity for TEAD. Furthermore, using a GAL4 reporter system and GAL4 fusions of TEAD1, TEAD2, TEAD3, and TEAD4, we demonstrated that CPD3.1 inhibited YAP-induced activity of all four TEAD isoforms with a similar potency (IC_{50} of 40, 33, 48, and 35 μM for TEAD1−4, respectively), demonstrating its pan-TEAD inhibitory activity. This likely reflects the high degree of sequence conservation in amino acids that form this pocket in all four TEAD isoforms. Importantly, CPD3.1 did not inhibit the activity of two TEAD-independent promoters or the endogenous mRNA expression of several TEAD-independent housekeeping genes, indicating specific inhibition of TEAD-dependent transcription.

The current lack of detailed knowledge of the cellular functions of each TEAD paralog means that it is unclear whether therapeutically useful TEAD inhibitors will be needed to target specific individual TEAD isoforms. Whether there is sufficient chemical and structural diversity in the YAP binding pocket to allow for paralog-selective inhibitors remains to be determined. YAP residues, essential for TEAD binding, that interact with this pocket are also conserved in TAZ, and the TAZ−TEAD4 crystal structure[62] indicates that TAZ can bind in a similar manner to YAP. It is also important to consider the wide-ranging biological functions of TEAD transcription factors, which have been shown to regulate diverse cellular functions, including osteoclastogenesis,[63] myoblast differentiation,[64] and cell fate decisions.[65] This may suggest that future pan-TEAD inhibiting therapies may be limited by undesirable side effects. However, this highlights the need for more research to dissect the specific function of individual TEAD proteins and the developments of TEAD isoform-specific inhibitors.

In summary, we report the identification of a novel YAP−TEAD protein−protein interaction inhibitor that inhibits TEAD activity, TEAD target gene expression, cell proliferation, and cell migration. We also describe the active fragment of this compound that retains all of these inhibitory properties. We suggest that this compound may aid the development of future lead compounds representing potent and selective TEAD inhibitors. Such compounds should be useful for the development of new therapies for the treatment of hyperproliferative cardiovascular diseases and patients who harbor cancers with amplified or overexpressed YAP, TAZ, or TEAD genes.

EXPERIMENTAL SECTION

BUDE in Silico Molecular Docking. In silico molecular docking was performed using the Bristol University Docking Engine (BUDE)[56,57] to dock conformers generated from the ZINC database into the YAP binding site of TEAD (3KYS.pdb). Briefly, the BUDE search area was defined as a 15 × 15 × 15 $Å^3$ grid centered on the epsilon 2 carbon atom of the YAP phenylalanine 95 residues (see Supplement Figure 1). Only TEAD1 atoms within 20 Å of this carbon atom were included in the docking analysis. A library of >8 million compounds, obtained from the clean, druglike subset of the ZINC8 database, was used for docking studies. Multiple conformers (approximately 20 per compound) of these compounds were generated using Confort (Certara Inc.), resulting in a library of

DOI: 10.1021/acs.jmedchem.8b01402
J. Med. Chem. 2019, 62, 1291−1305

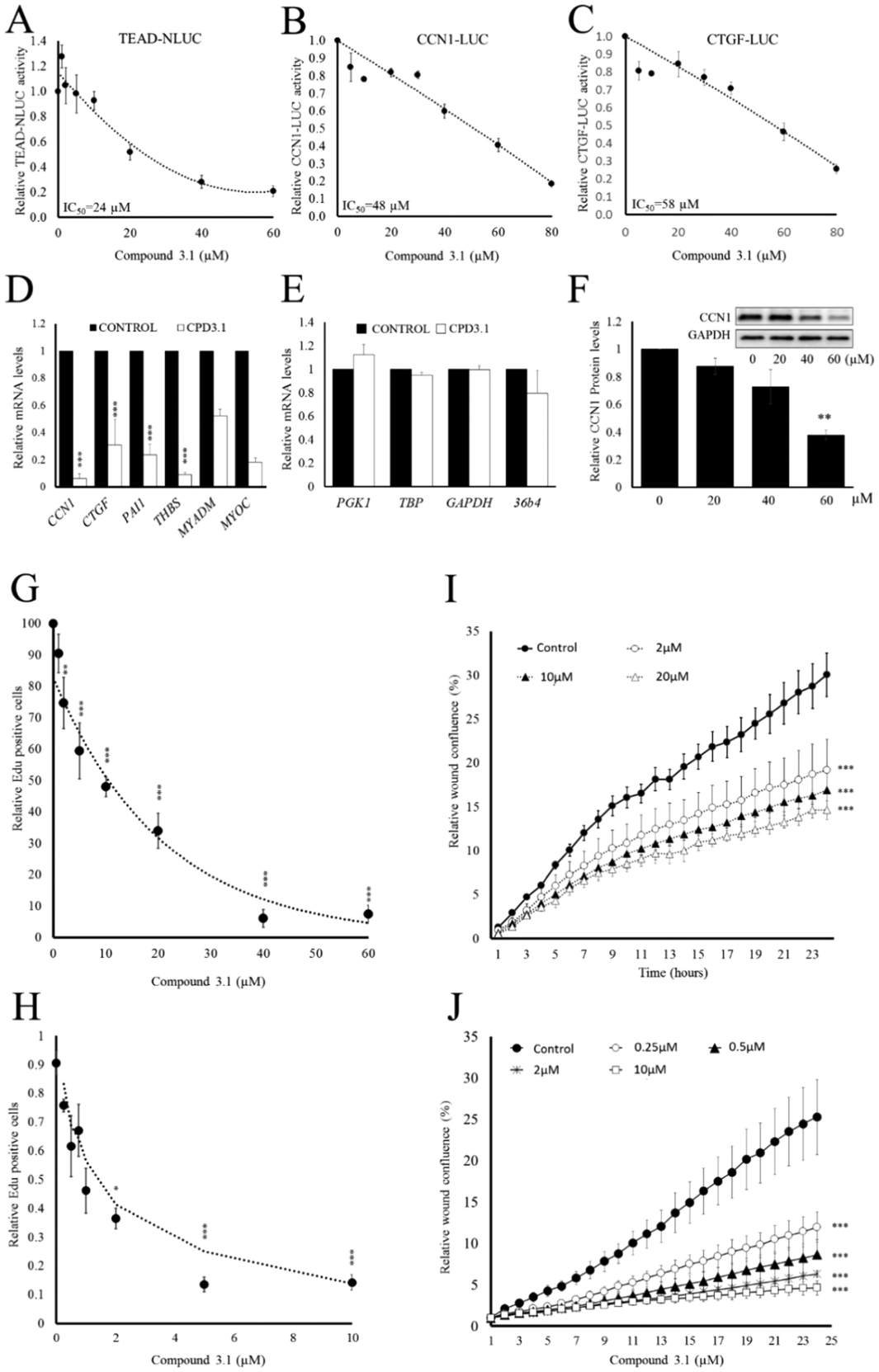

Figure 9. Compound 3.1 inhibits TEAD target gene expression, cell proliferation, and cell migration in RaVSMCs. RaVSMCs stably transduced with TEAD-NLUC (A) or transiently transfected with *CCN1*-LUC or *CTGF*-LUC were treated with the indicated concentrations of compound 3.1 for 6 hr. Cell conditioned media (A) or cell lysates (B−C) were assayed for nanoluciferase or fire-fly luciferase activity, respectively. VSMC were treated with 60 μM compound 3.1 for 6 h (n = 3). Total RNA was analyzed for mRNA levels of TEAD-target genes (D) or constitutive housekeeping genes (E) by qRT-PCR. VSMC were treated with indicated concentrations of compound 3.1 for 16 hr (n = 4). Total cell lysates were analyzed for *CCN1* protein expression by Western blotting (F). RaVSMCs (G) or HuVSMC (H) were treated with indicated concentrations of

DOI: 10.1021/acs.jmedchem.8b01402
J. Med. Chem. 2019, 62, 1291−1305

Figure 9. continued

compound 3.1 for 18 h followed by labeling in 10 μM EdU for a further 6 h (n = 4). RaVSMCs (I) or HuVSMC (J) were treated with indicated concentrations of compound 3.1 and cell migration quantified using IncuCyte real time migration assay (n = 4).

approximately 160 million distinct structures that was docked into the TEAD1 pocket that forms the YAP−TEAD interaction interface 3.[51] Each conformer was docked using 20 000 randomly generated "poses" within the search space and the free energy of binding between the conformer and TEAD calculated. The 1000 poses with the lowest energies were selected and randomly "mutated" with X, Y, and Z axis translations and rotations to generate a new generation of 20 000 poses. Ten generations of this docking algorithm were performed, resulting in an optimized docking pose for each conformer and a list of all 160 million conformers ranked by predicted free energy of binding. The top 100 000 ranked compound conformers with the lowest binding energies were selected and docked with five conformers of TEAD1. The top 1000 compound conformers with the lowest binding energies for each TEAD conformer were selected, and compound conformers that appeared in at least four of the list were identified (Supplement Data File S1). This resulted in 3.85% of compound conformers (representing 91 distinct compounds) being shortlisted (Supplement Figure 1). Of these 91 compounds, only 38 (41.75%) were commercially available (Supplement Figure 2). These 38 compounds were manually curated for chemical diversity and 16 selected for testing. Shortlisted hits were screened for pan assay interference compounds (PAINS) using the online PAINS filters at http://zinc15.docking.org/patterns/home/ and http://www.cbligand.org/PAINS/. Hit compounds passed both filters.

Modeling Methods. The TEAD/YAP complex crystal structure (3KYS.pdb) was used as the basis for the 100 ns dynamics simulations of the apo TEAD protein. The GROMACS 5.1.2.[66] software suite with the Amber99-SB-ILDN[67] force field was used to generate multiple TEAD conformers. Five frames were chosen, representing the greatest RMSD across the trajectory.

Molecular graphics manipulations and visualizations were performed using VMD-1.9.1 and Chimera-1.10.2.[68] Pdb2gmx was used to prepare the assembly. Hydrogen atoms were added consistent with pH 7. The system was surrounded by a box extending 2 nm from the peptide (in each axis) and filled with TIP3P water. The random water molecules were replaced by sodium and chloride ions to give a neutral (uncharged overall) box and an ionic strength of 0.15 M. The system was energy-minimized for 5000 steps prior to position-restrained and subsequent unrestrained, molecular dynamics simulations.

Simulation Details. All simulations were performed as NPT (standard state) ensembles at 310 K using periodic boundary conditions. Short-range electrostatic and van der Waals interactions were truncated at 1.4 nm, while long-range electrostatics were treated with the particle mesh Ewald's method and a long-range dispersion correction applied. Pressure was controlled by the Parrinello−Rahman barostat and temperature by the Nosé−Hoover thermostat. The simulations were integrated with a leap-frog algorithm over a 2 fs time step, constraining bond vibrations with the P-LINCS method. Structures were saved every 0.1 ns for analysis and run over 100 ns. Simulation data were accumulated on BlueCrystal, the University of Bristol's high-performance computing machine.

Compound Selection for Testing in Vitro. The output from the initial BUDE docking process provided poses and predicted binding energies for all conformers. These were analyzed and sorted according to binding energy. The top 100 000 most favored binders were redocked into multiple conformers of the TEAD protein. These were again analyzed and ranked, and the compounds that had the best predicted binding energies and that performed consistently across all docks were selected for purchase (Supplement Table 1).

Compounds. Unless otherwise stated, all screening compounds were purchased from Molport (Latvia). Compound 3.1 was purchased from Fluorochem (U.K.). Compounds 3.2 and 3.3 were purchased from Sigma-Aldrich (U.K.). All compounds were dissolved in dimethyl sulfoxide at a concentration of either 10 or 20 mM. Respective order numbers and ZINC IDs for all compounds are described in Supplement Table 2. Commercially obtained test compounds had >95% purity and were not purified further. Compound purity was confirmed by ^{1}H NMR spectroscopy (Supplement Figure 9).

Cell Culture. HeLa cells were purchased from the American Tissue Culture Collection (ATCC) and cultured in Dulbecco's modified Eagle's medium (DMEM) supplemented with 10% fetal bovine serum, 100 U/mL penicillin, 100 U/mL streptomycin, and 2 mM L-glutamine. Vascular smooth muscle cells (VSMCs) were isolated from the thoracic aortas of male Sprague-Dawley rats killed by cervical dislocation in accordance with the Directive 2010/63/EU of the European Parliament. Approval was granted by the University of Bristol ethical review board. Cultures of rat aortic VSMCs (RaVSMCs) were performed in 10% fetal calf serum/DMEM unless otherwise stated.

In Vitro GST−TEAD−YAP Interaction Assays. The DNA fragment encoding human TEAD1 (corresponding to residues 194−411) was amplified by polymerase chain reaction (PCR) and cloned into the BamH1 and EcoR1 sites of vector pGEX-6P1, in frame with the terminal GST tag. GST−TEAD1 fusion protein expression was induced in SoluBL21s *Escherichia coli* by culture at 25 °C in the presence of 0.2 mM IPTG for 18 h. GST−TEAD1 protein was bound to glutathione resin (GE Healthcare), and 25 μL of beads (containing approximately 5 μg of GST−TEAD1) was used to affinity-isolate endogenous human YAP protein from HEK293 cell lysate by incubation at 4 °C for 18 h in binding buffer (10 mM Tris pH 8.0, 150 mM NaCl, 10 mM $MgCl_2$, 5% glycerol, 0.5% Triton-X-100) in the presence of 200 μM of the indicated compound. Bound proteins were eluted by boiling in Laemmli sample buffer and YAP and GST−TEAD levels quantified by Western blotting with an anti-YAP antibody (Cell Signaling; #4912) and an anti-GST antibody (Cell Signaling; #5475S).

Co-immunoprecipitation and YAP−TEAD Interaction Assays. HeLa cells were transiently transfected with either pRK5-myc-TEAD1 (Addgene #33109) or pEGFP-C3-YAP1 (Addgene #17843). These plasmids express human TEAD1 protein fused to the myc-epitope-tag amino acid sequence (amino acids: EQKLISEEDL) or YAP1 fused to enhanced green fluorescent protein, respectively. Cytosolic extracts were prepared in 10 mM Tris pH 7.6, 10 mM KCl, 0.5 mM ethylenediaminetetraacetic acid (EDTA), and 0.2% NP-40. Nuclei were pelleted and extracted in half volume of 10 mM Tris pH 7.6, 10 mM KCl, 450 mM NaCl, 0.5 mM dithiothreitol, and 0.5 mM EDTA and pooled with the cytosolic extracts. Myc-TEAD-containing extracts were incubated on ice for 30 min with 200 μM CPD3. An equal volume of GFP−YAP-containing lysate was added and incubated for a further 30 min on ice. GFP−YAP or myc-TEAD1 was immunoprecipitated, as indicated, using GFP-Trap or Myc-Trap beads (Chromotek), respectively. Following washing, immunoprecipitated proteins were eluted by boiling in sodium dodecyl sulfate (SDS) buffer (50 mM Tris pH 6.8, 20% glycerol, 2% SDS) and analyzed by Western blotting.

YAP−TEAD interaction assays were performed in 96-well protein-G-coated plates (Pierce) by capturing myc-TEAD1 from cell lysates of HeLa cells transiently transfected with pRK5-myc-TEAD1 plasmid with an anti-myc tag antibody (Thermo Fisher Scientific; clone 9E10). Plates with immobilized myc-TEAD were pretreated with indicated concentrations of compound in phosphate-buffered saline (PBS) for 1 h at 4 °C before co-incubation with lysate from HeLa cells transiently transfected with a plasmid expressing YAP−nanoluciferase fusion protein (YAP−NL). Following four washes in PBS, bound YAP−NL was detected and quantified by incubation with NanoGlo assay buffer (Figure 1G).

DOI: 10.1021/acs.jmedchem.8b01402
J. Med. Chem. 2019, 62, 1291−1305

Reporter Gene Activity Assays. Compounds were initially screened for ability to inhibit TEAD-dependent transcriptional activity in HeLa cells transduced with a lentiviral vector expressing secreted nanoluciferase under the control of multimerized TEAD consensus elements (5′-CACATTCCA-3′). 8xTEAD NanoLuc was generated by cloning the 8xTEAD promoter from the 8xTEAD-Luc plasmid (Addgene #34615) into the pENTR gateway entry vector (Promega). This was then recombined into pLNT-sec-Nluc-2A-eGFP destination vector (supplied by Tristan McKay; University of Manchester). Lentiviruses were generated by Viafect-mediated co-transfection of pLNT8x-TEAD-sec-Nluc-2A-eGFP, Δ8.9, and VSV-G vectors into HEK293T cells (ATCC), and lentiviral-containing culture supernatants were used to infect HeLa cells in the presence of 6 μg/mL polybrene. For compound screening, 8xTEAD NanoLuc-transduced HeLa cells were seeded at 2×10^4 cells/well in 96-well plates. After 48 h, the cells were washed in PBS and incubated with test compounds at the indicated concentrations for 2 h. The cells were washed again in PBS and incubated with the compound for a further 4 h. Conditioned culture medium (50 μL) was assayed for secreted nanoluciferase activity using NanoGlo activity assays kit (Promega) and a Glomax Discover luminometer.

TNT1-minP reporter containing the Troponin-T minimal promoter was generated by digesting 8xGTIIC-luciferase plasmid (Addgene #34615) with *Kpn1* and *BglII* to remove the TEAD elements, followed by blunt end re-ligation. A 2.177 kb fragment of the human *CCN1* promoter containing two proximal TEAD elements (Hg19;chr1:86044316−chr1:86046493) was described previously[39] and cloned into pGL4-luciferase (Promega). The proximal promoter regions of the *CTGF* (Hg19;chr6:132272455−132272687) promoter, containing a consensus TEAD-binding element, was amplified by PCR from human genomic DNA and cloned into the Kpn1 and Nhe1 sites of pGL4-luciferase. The cells were transfected with firefly luciferase reporter plasmids using a Nuceofector 1.5 (Lonza). Cell lysates were assayed for luciferase activity using the luciferase assay system (Promega). GAL4-Nano-luciferase plasmid (GLA4-NLUC) was created by subcloning the 5xGAL4 binding elements from plasmid pG5E1b-LUC (a gift from Ugo Moens, University of Tromsø, Norway) into the Nhe1 and Xho1 sites of pNL3.3[*sec-Nluc*/minP] (Promega). Plasmids expressing GAL4 fusions of TEAD1 (#33108), TEAD2 (#33107), TEAD3 (#33106), and TEAD4 (#33105) and FLAG-YAP (#18881) were obtained from Addgene.

Cell Viability Assay. Cell viability was quantified using the live/dead viability/cytotoxicity assay standard protocol (Invitrogen). Maximum cell death was quantified by incubating cells for 10 min with 0.1% Triton-X, followed by incubation with 0.4 μM ethidium homodimer-1 for an additional 10 min. Fluorescence was measured using a GloMax Discover multiplate reader (Promega).

Proliferation and Real-Time Scratch Wound Migration Assays. Cell proliferation was measured using the Click-iT EdU 488 assay (Sigma-Aldrich). Briefly, the cells were treated with indicated concentrations of compounds for 24 h with the last 4 h being in the presence of 10 μM EdU. The cells were fixed in 4% formaldehyde and stained for EdU incorporation, following the kit's standard protocol. The cells were counterstained with Hoechst 33342 nucleic acid for 20 min. Fluorescent images of at least three fields of view per well were counted using ImageJ software. Real-time analysis of cell migration was performed using an IncuCyte ZOOM live cell imaging system (Essen BioScience) according to the manufacturer's instructions. Briefly, the cells were seeded (1.2×10^4 cells/well for HeLa cells, 1.5×10^4 cells/well for RaVSMCs, and 1×10^4 cells/well) into ImageLock 96-well plates. After 36 h, the cells were pretreated overnight with indicated concentrations of compounds. The wells were scratched using a WoundMaker tool, and the media were replaced containing test compounds. Phase contrast images of cell migration into the wounded area were acquired hourly for 24 h. Relative wound confluence was calculated using the Cell Migration Image analysis module of the IncuCyte ZOOM software.

Quantitative reverse transcription (RT)-PCR: quantification of mRNA was performed by RT-qPCR, as described previously.[39] Total RNA was extracted using Ambion PureLink kits (Thermo Fisher) and reverse-transcribed using QuantiTect RT kit (Qiagen) and random primers. Quantitative PCR was performed using Roche SYBR Green using a Qiagen Roto-GeneRotor-Gene Q PCR machine (20 seconds@95 °C; 20 seconds @62 °C; 20 seconds@72 °C). Data were normalized to nonstimulated controls. Primer sequences are described in Supplement Table 2.

Western Blotting. Extracted samples were separated by 4−12% SDS-polyacrylamide gel electrophoresis (Bio-Rad) and transferred to poly(vinylidene difluoride) membranes (GE Healthcare). Membranes were blocked in 5% low-fat milk in 10 mM Tris pH 7.6, 150 mM NaCl, 0.2% Tween. Antibodies YAP (1:1000, Cell Signaling; 4912S), CCN1 (1:1000, R&D Systems; AF6009), GAPDH (1:10 000, Millipore; MAB374), and GST (1:1000, Cell Signaling; 5475S), for GST-tagged TEAD detection, were incubated overnight in 5% bovine serum albumin in 10 mM Tris pH 7.6, 150 mM NaCl, 0.2% Tween, followed by probing with a relevant secondary antibody and developed using ChemiDoc-MP imaging system (Bio-Rad).

Saturation Transfer Diffusion Nuclear Magnetic Resonance (STD NMR) Analysis. Binding of compounds to human TEAD was performed using STD NMR analysis. Briefly, TEAD1 protein (residues 194−411) was prepared by solution cleavage of the GST tag from recombinant GST−TEAD1 (194−411). GST−TEAD1 protein was eluted from glutathione beads by 40 mM reduced glutathione. GST tag was removed by incubation with PreScission protease (Sigma-Aldrich) at 4 °C for 18 h. Glutathione was removed by dialysis against 1000 volumes of 1× PBS at 4 °C for 4 h. Free GST protein was removed by incubation with glutathione resin. All NMR spectroscopy experiments were performed on a Bruker Avance III HD 700 MHz spectrometer equipped with a 1.7 mm inverse triple-resonance microcryocoil probe. NMR samples were prepared in 40 μL with PBS pH 7.4 in 60% D_2O (uncorrected for D_2O). TEAD (20 mM) was used with a final concentration of 2 mM compound. For the STD experiments, the standard Bruker stddiffesgp.3 pulse sequence was used with a saturation time of 7 s and a spectral width of 15.9 ppm with eight scans. The on-resonance frequency was set to 0.85 ppm, while the off-resonance frequency was set to −28 ppm. Appropriate blank experiments, in the absence of protein or ligand, were performed to test the lack of direct saturation to the ligand protons.

Statistical Analysis. Unless otherwise stated, data are presented as mean ± standard error and analyzed by one-way analysis of variance with Dunnett's multiple comparison test for multiple comparisons. * indicates $p < 0.05$, ** indicates $p < 0.01$, and *** indicates $p < 0.001$.

■ ASSOCIATED CONTENT

Supporting Information

The Supporting Information is available free of charge on the ACS Publications website at DOI: 10.1021/acs.jmedchem.8b01402.

ZINC ID lists; primers designed for use in qRT-PCR assays; properties of compounds (Supplement Tables 1−3); overview of BUDE in silico molecular docking; Venn diagrams; effect of shortlisted compounds on cell viability; effect of CPD3 on TEAD-target gene mRNA levels in RaVSMCs; effect of low micromolar doses of CPD3 on rat VSMC migration; effect of CPD3, CPD3.1, CPD3.2 and CPD3.3 on cell viability; CPD3 and CPD3.1 do not nonspecifically inhibit nanoluciferase activity; isothermal titration calorimetric estimation; schematic representation of GAL4−TEAD fusion protein reporter assay; effect of compound 3.1 on *TNNT*-minimal promoter-LUC activity; dose repose analysis; effect of CPD3.1 on the proliferation of the TEAD-independent MCF7 cell line; ^1H NMR spectra; schematic illustration of YAP-TEAD-dependent regu-

DOI: 10.1021/acs.jmedchem.8b01402
J. Med. Chem. 2019, 62, 1291−1305

lation of pro-mitogenic and pro-migratory genes (Supplement Figures 1−14) (PDF)
Molecular formula strings (CSV)
Ranked list of BUDE screen hits (CSV)
BUDE docking data (Supplement Data File S1) (XLSX)
TEAD1 PDB file used for BUDE docking (PDB)
Compound 3 (CPD3) PDB file (PDB)
Compound 3.1 (CPD3.1) PDB file (PDB)

AUTHOR INFORMATION

Corresponding Author

*E-mail: mark.bond@bristol.ac.uk. Tel: +44 (0)117 3423586.

ORCID

Richard B. Sessions: 0000-0003-0320-0895
Christopher Williams: 0000-0001-5806-9842
Matthew P. Crump: 0000-0002-7868-5818
Mark Bond: 0000-0003-2788-278X

Author Contributions

S.A.S. performed BUDE docking studies, the majority of experimental work, and co-wrote the manuscript; R.B.S. and D.K.S. performed BUDE docking studies; C.W. performed NMR studies; M.C.M. performed proliferation assays; M.P.C. helped with NMR studies; T.R.M. provided lentiviral reporter vectors; R.E. performed reporter experiments; G.H. performed ITC analysis; A.C.N. helped obtain funding and manuscript preparation; and M.B. conceived the study, obtained funding, performed some experiments, and wrote the manuscript.

Notes

The authors declare no competing financial interest.

ACKNOWLEDGMENTS

This work was supported by the British Heart Foundation project grant PG/15/100/31877. The authors acknowledge BrisSynBio, a BBSRC/EPSRC Synthetic Biology Research Center for access to the BBSRC/EPSRC-funded 700 MHz NMR spectrometer {BB/LO1386X/1}. T.R.M. received funding from the European Union Horizon2020 grant BATCure Ref: 666918. The authors acknowledge funding support from the NIHR Biomedical Research Centre at University Hospitals Bristol NHS Foundation Trust and University of Bristol. The views expressed in this publication are those of the authors and not necessarily those of the NHS, the National Institute for Health Research, or the Department of Health and Social Care.

ABBREVIATIONS

BUDE, Bristol University Docking Engine; GST, glutathione S transferase; NLUC, nanoluciferase; NMR, nuclear magnetic resonance; PBS, phosphate-buffered saline; RMSD, root-mean-square deviation; RNA, ribonucleic acid; SRF, serum response factor; STD, saturation transfer diffusion; TAZ, transcriptional coactivator with PDZ-binding motif; TEAD, TEA domain transcription factor 1; YAP, Yes-associated protein; VSMC, vascular smooth muscle cell

REFERENCES

(1) Zhao, B.; Ye, X.; Yu, J. D.; Li, L.; Li, W. Q.; Li, S. M.; Yu, J. J.; Lin, J. D.; Wang, C. Y.; Chinnaiyan, A. M.; Lai, Z.-C.; Guan, K.-L. TEAD mediates YAP-dependent gene induction and growth control. *Genes Dev.* **2008**, *22*, 1962−1971.

(2) Ota, M.; Sasaki, H. Mammalian TEAD proteins regulate cell proliferation and contact inhibition as transcriptional mediators of HIPPO signaling. *Development* **2008**, *135*, 4059−4069.

(3) Tsai, C. R.; Anderson, A. E.; Burra, S.; Jo, J.; Galko, M. J. Yorkie regulates epidermal wound healing in Drosophila larvae independently of cell proliferation and apoptosis. *Dev. Biol.* **2017**, *427*, 61−71.

(4) Chen, Z.; Friedrich, G. A.; Soriano, P. Transcriptional enhancer factor-1 disruption by a retroviral gene trap leads to heart-defects and embryonic lethality in mice. *Genes Dev.* **1994**, *8*, 2293−2301.

(5) Yagi, R.; Kohn, M. J.; Karavanova, I.; Kaneko, K. J.; Vullhorst, D.; DePamphilis, M. L.; Buonanno, A. Transcription factor TEAD4 specifies the trophectoderm lineage at the beginning of mammalian development. *Development* **2007**, *134*, 3827−3836.

(6) Wang, C. Y.; Nie, Z.; Zhou, Z. M.; Zhang, H. L.; Liu, R.; Wu, J.; Qin, J. Y.; Ma, Y.; Chen, L.; Li, S. M.; Chen, W. L.; Li, F. B.; Shi, P. G.; Wu, Y. Y.; Shen, J.; Chen, C. S. The interplay between TEAD4 and KLF5 promotes breast cancer partially through inhibiting the transcription of p27(Kip1). *Oncotarget* **2015**, *6*, 17685−17697.

(7) Nowee, M. E.; Snijders, A. M.; Rockx, D. A. P.; de Wit, R. M.; Kosma, V. M.; Hamalainen, K.; Schouten, J. P.; Verheijen, R. H. M.; van Diest, P. J.; Albertson, D. G.; Dorsman, J. C. DNA profiling of primary serous ovarian and fallopian tube carcinomas with array comparative genomic hybridization and multiplex ligation-dependent probe amplification. *J. Pathol.* **2007**, *213*, 46−55.

(8) Skotheim, R. I.; Autio, R.; Lind, G. E.; Kraggerud, S. M.; Andrews, P. W.; Monni, O.; Kallioniemi, O.; Lothe, R. A. Novel genomic aberrations in testicular germ cell tumors by array-CGH, and associated gene expression changes. *Cell. Oncol.* **2006**, *28*, 315−326.

(9) Schütte, U.; Bisht, S.; Heukamp, L. C.; Kebschull, M.; Florin, A.; Haarmann, J.; Hoffmann, P.; Bendas, G.; Buettner, R.; Brossart, P.; Feldmann, G. HIPPO signaling mediates proliferation, invasiveness, and metastatic potential of clear cell renal cell carcinoma. *Transl. Oncol.* **2014**, *7*, 309−321.

(10) Fernandez-L, A.; Northcott, P. A.; Dalton, J.; Fraga, C.; Ellison, D.; Angers, S.; Taylor, M. D.; Kenney, A. M. YAP1 is amplified and up-regulated in hedgehog-associated medulloblastomas and mediates Sonic hedgehog-driven neural precursor proliferation. *Genes Dev.* **2009**, *23*, 2729−2741.

(11) Zhou, G. X.; Li, X. Y.; Zhang, Q.; Zhao, K.; Zhang, C. P.; Xue, C. H.; Yang, K.; Tian, Z. B. Effects of the HIPPO signaling pathway in human gastric cancer. *Asian Pac. J. Cancer Prev.* **2013**, *14*, 5199−5205.

(12) Chan, S. W.; Lim, C. J.; Loo, L. S.; Chong, Y. F.; Huang, C. X.; Hong, W. J. TEADs mediate nuclear retention of TAZ to promote oncogenic transformation. *J. Biol. Chem.* **2009**, *284*, 14347−14358.

(13) Zhao, B.; Li, L.; Lei, Q. Y.; Guan, K. L. The Hippo-YAP pathway in organ size control and tumorigenesis: an updated version. *Genes Dev.* **2010**, *24*, 862−874.

(14) Liu-Chittenden, Y.; Huang, B.; Shim, J. S.; Chen, Q.; Lee, S. J.; Anders, R. A.; Liu, J. O.; Pan, D. J. Genetic and pharmacological disruption of the TEAD-YAP complex suppresses the oncogenic activity of YAP. *Genes Dev.* **2012**, *26*, 1300−1305.

(15) Lim, B.; Park, J. L.; Kim, H. J.; Park, Y. K.; Kim, J. H.; Sohn, H. A.; Noh, S. M.; Song, K. S.; Kim, W. H.; Kim, Y. S.; Kim, S. Y. Integrative genomics analysis reveals the multilevel dysregulation and oncogenic characteristics of TEAD4 in gastric cancer. *Carcinogenesis* **2014**, *35*, 1020−1027.

(16) Liu, Y.; Wang, G.; Yang, Y.; Mei, Z.; Liang, Z.; Cui, A.; Wu, T.; Liu, C. Y.; Cui, L. Increased TEAD4 expression and nuclear localization in colorectal cancer promote epithelial-mesenchymal transition and metastasis in a YAP-independent manner. *Oncogene* **2016**, *35*, 2789−2800.

(17) Knight, J. F.; Shepherd, C. J.; Rizzo, S.; Brewer, D.; Jhavar, S.; Dodson, A. R.; Cooper, C. S.; Eeles, R.; Falconer, A.; Kovacs, G.; Garrett, M. D.; Norman, A. R.; Shipley, J.; Hudson, D. L. TEAD1 and c-Cbl are novel prostate basal cell markers that correlate with poor clinical outcome in prostate cancer. *Br. J. Cancer* **2008**, *99*, 1849−1858.

(18) Wang, X. B.; Hu, G. Q.; Gao, X. W.; Wang, Y.; Zhang, W.; Harmon, E. Y.; Zhi, X.; Xu, Z. P.; Lennartz, M. R.; Barroso, M.;

DOI: 10.1021/acs.jmedchem.8b01402
J. Med. Chem. 2019, 62, 1291−1305

Trebak, M.; Chen, C. S.; Zhou, J. L. The Induction of Yes-Associated Protein Expression after Arterial Injury Is Crucial for Smooth Muscle Phenotypic Modulation and Neointima Formation. *Arterioscler., Thromb., Vasc. Biol.* **2012**, *32*, 2662−2669.
(19) Vassilev, A.; Kaneko, K. J.; Shu, H. J.; Zhao, Y. M.; DePamphilis, M. L. TEAD/TEF transcription factors utilize the activation domain of YAP65, a Src/Yes-associated protein localized in the cytoplasm. *Genes Dev.* **2001**, *15*, 1229−1241.
(20) Vaudin, P.; Delanoue, R.; Davidson, I.; Silber, J.; Zider, A. TONDU (TDU), a novel human protein related to the product of vestigial (vg) gene of *Drosophila melanogaster* interacts with vertebrate TEF factors and substitutes for Vg function in wing formation. *Development* **1999**, *126*, 4807−4816.
(21) Helias-Rodzewicz, Z.; Perot, G.; Chibon, F.; Ferreira, C.; Lagarde, P.; Terrier, P.; Coindre, J. M.; Aurias, A. YAP1 and VGLL3, encoding two cofactors of TEAD transcription factors, are amplified and overexpressed in a subset of soft tissue sarcomas. *Genes, Chromosomes Cancer* **2010**, *49*, 1161−1171.
(22) Pobbati, A. V.; Hong, W. J. Emerging roles of TEAD transcription factors and its coactivators in cancers. *Cancer Biol. Ther.* **2013**, *14*, 390−398.
(23) Belandia, B.; Parker, M. G. Functional interaction between the p160 coactivator proteins and the transcriptional enhancer factor family of transcription factors. *J. Biol. Chem.* **2000**, *275*, 30801−30805.
(24) Hao, Y. W.; Chun, A.; Cheung, K.; Rashidi, B.; Yang, X. L. Tumor suppressor LATS1 is a negative regulator of oncogene YAP. *J. Biol. Chem.* **2008**, *283*, 5496−5509.
(25) Zhao, B.; Wei, X.; Li, W.; Udan, R. S.; Yang, Q.; Kim, J.; Xie, J.; Ikenoue, T.; Yu, J.; Li, L.; Zheng, P.; Ye, K.; Chinnaiyan, A.; Halder, G.; Lai, Z. C.; Guan, K. L. Inactivation of YAP oncoprotein by the Hippo pathway is involved in cell contact inhibition and tissue growth control. *Genes Dev.* **2007**, *21*, 2747−2761.
(26) Dong, J. X.; Feldmann, G.; Huang, J. B.; Wu, S.; Zhang, N. L.; Comerford, S. A.; Gayyed, M. F.; Anders, R. A.; Maitra, A.; Pan, D. J. Elucidation of a universal size-control mechanism in Drosophila and mammals. *Cell* **2007**, *130*, 1120−1133.
(27) Zhang, H. B.; Ramakrishnan, S. K.; Triner, D.; Centofanti, B.; Maitra, D.; Gyorffy, B.; Sebolt-Leopold, J. S.; Dame, M. K.; Varani, J.; Brenner, D. E.; Fearon, E. R.; Omary, M. B.; Shah, Y. M. Tumor-selective proteotoxicity of verteporfin inhibits colon cancer progression independently of YAP1. *Sci. Signaling* **2015**, *8*, No. ra98.
(28) Yu, F. X.; Zhao, B.; Guan, K. L. HIPPO pathway in organ size control, tissue homeostasis, and cancer. *Cell* **2015**, *163*, 811−828.
(29) Lee, M. J.; Byun, M. R.; Furutani-Seiki, M.; Hong, J. H.; Jung, H. S. YAP and TAZ regulate skin wound healing. *J. Invest. Dermatol.* **2014**, *134*, 518−525.
(30) Juan, W.; Hong, W. Targeting the HIPPO signaling pathway for tissue regeneration and cancer therapy. *Genes* **2016**, *7*, 55.
(31) Zanconato, F.; Cordenonsi, M.; Piccolo, S. YAP/TAZ at the roots of cancer. *Cancer Cell* **2016**, *29*, 783−803.
(32) Cao, L. Q.; Sun, P. L.; Yao, M.; Jia, M.; Gao, H. W. Expression of YES-associated protein (YAP) and its clinical significance in breast cancer tissues. *Hum. Pathol.* **2017**, *68*, 166−174.
(33) Xia, Y.; Chang, T.; Wang, Y.; Liu, Y.; Li, W.; Li, M.; Fan, H.-Y. YAP promotes ovarian cancer cell tumorigenesis and is indicative of a poor prognosis for ovarian cancer patients. *PLoS One* **2014**, *9*, No. e91770.
(34) Wang, L. J.; Shi, S. J.; Guo, Z. Y.; Zhang, X.; Han, S. X.; Yang, A. G.; Wen, W. H.; Zhu, Q. Overexpression of YAP and TAZ is an independent predictor of prognosis in colorectal cancer and related to the proliferation and metastasis of colon cancer cells. *PLoS One* **2013**, *8*, No. e65539.
(35) Wang, Y. P.; Tang, D. X. Expression of Yes-associated protein in liver cancer and its correlation with clinicopathological features and prognosis of liver cancer patients. *Int. J. Clin. Exp. Med.* **2015**, *8*, 1080−1086.
(36) Allende, M. T. S.; Zeron-Medina, J.; Hernandez, J.; et al. Overexpression of yes associated protein 1, an independent prognostic marker in patients with pancreatic ductal adenocarcinoma, correlated with liver metastasis and poor prognosis. *Pancreas* **2017**, *46*, 913−920.
(37) Zhao, B.; Ye, X.; Yu, J.; Li, L.; Li, W.; Li, S.; Yu, J.; Lin, J. D.; Wang, C.-Y.; Chinnaiyan, A. M.; Lai, Z.-C.; Guan, K.-L. TEAD mediates YAP-dependent gene induction and growth control. *Genes Dev.* **2008**, *22*, 1962−1971.
(38) Zhi, X.; Zhao, D.; Zhou, Z. M.; Liu, R.; Chen, C. S. YAP promotes breast cell proliferation and survival partially through stabilizing the KLF5 transcription factor. *Am. J. Pathol.* **2012**, *180*, 2452−2461.
(39) Kimura, T. E.; Duggirala, A.; Smith, M. C.; White, S.; Sala-Newby, G. B.; Newby, A. C.; Bond, M. The Hippo pathway mediates inhibition of vascular smooth muscle cell proliferation by cAMP. *J. Mol. Cell. Cardiol.* **2016**, *90*, 1−10.
(40) Wang, C.; Zhu, X. Y.; Feng, W. W.; Yu, Y. H.; Jeong, K. J.; Guo, W.; Lu, Y. L.; Mills, G. B. Verteporfin inhibits YAP function through up-regulating 14-3-3 sigma sequestering YAP in the cytoplasm. *Am. J. Cancer Res.* **2016**, *6*, 27−37.
(41) Yu, F. X.; Zhao, B.; Panupinthu, N.; Jewell, J. L.; Lian, I.; Wang, L. H.; Zhao, J. G.; Yuan, H. X.; Tumaneng, K.; Li, H. R.; Fu, X. D.; Mills, G. B.; Guan, K. L. Regulation of the HIPPO-YAP pathway by G-protein-coupled receptor signaling. *Cell* **2012**, *150*, 780−791.
(42) Fan, R.; Kim, N. G.; Gumbiner, B. M. Regulation of Hippo pathway by mitogenic growth factors via phosphoinositide 3-kinase and phosphoinositide-dependent kinase-1. *Proc. Natl. Acad. Sci. U.S.A.* **2013**, *110*, 2569−2574.
(43) Park, H. W.; Kim, Y. C.; Yu, B.; Moroishi, T.; Mo, J. S.; Plouffe, S. W.; Meng, Z. P.; Lin, K. C.; Yu, F. X.; Alexander, C. M.; Wang, C. Y.; Guan, K. L. Alternative Wnt signaling activates YAP/TAZ. *Cell* **2015**, *162*, 780−794.
(44) Dupont, S.; Morsut, L.; Aragona, M.; Enzo, E.; Giulitti, S.; Cordenonsi, M.; Zanconato, F.; Le Digabel, J.; Forcato, M.; Bicciato, S.; Elvassore, N.; Piccolo, S. Role of YAP/TAZ in mechanotransduction. *Nature* **2011**, *474*, 179−183.
(45) Gumbiner, B. M.; Kim, N. G. The Hippo-YAP signaling pathway and contact inhibition of growth. *J. Cell Sci.* **2014**, *127*, 709−717.
(46) Holden, J. K.; Cunningham, C. N. Targeting the HIPPO pathway and cancer through the TEAD family of transcription factors. *Cancers* **2018**, *10*, 81.
(47) Zhubanchaliyev, A.; Temirbekuly, A.; Kongrtay, K.; Wanshura, L. C.; Kunz, J. Targeting mechanotransduction at the transcriptional level: YAP and BRD4 are novel therapeutic targets for the reversal of liver fibrosis. *Front. Pharmacol.* **2016**, *7*, 462.
(48) Scott, D. E.; Bayly, A. R.; Abell, C.; Skidmore, J. Small molecules, big targets: drug discovery faces the protein-protein interaction challenge. *Nat. Rev. Drug Discovery* **2016**, *15*, 533−550.
(49) Dasari, V. R.; Mazack, V.; Feng, W.; Nash, J.; Carey, D. J.; Gogoi, R. Verteporfin exhibits YAP-independent anti-proliferative and cytotoxic effects in endometrial cancer cells. *Oncotarget* **2017**, *8*, 28628−28640.
(50) Oku, Y.; Nishiya, N.; Shito, T.; Yamamoto, R.; Yamamoto, Y.; Oyama, C.; Uehara, Y. Small molecules inhibiting the nuclear localization of YAP/TAZ for chemotherapeutics and chemosensitizers against breast cancers. *FEBS Open Bio* **2015**, *5*, 542−549.
(51) Li, Z.; Zhao, B.; Wang, P.; Chen, F.; Dong, Z. H.; Yang, H. R.; Guan, K. L.; Xu, Y. H. Structural insights into the YAP and TEAD complex. *Genes Dev.* **2010**, *24*, 235−240.
(52) Pobbati, A. V.; Han, X.; Hung, A. W.; Weiguang, S.; Huda, N.; Chen, G. Y.; Kang, C. B.; Chia, C. S. B.; Luo, X. L.; Hong, W. J.; Poulsen, A. Targeting the central pocket in human transcription factor TEAD as a potential cancer therapeutic strategy. *Structure* **2015**, *23*, 2076−2086.
(53) Halgren, T. A. Identifying and characterizing binding sites and assessing druggability. *J. Chem Inf. Model.* **2009**, *49*, 377−389.
(54) Zhang, Z. Z.; Lin, Z. H.; Zhou, Z.; Shen, H. C.; Yan, S. F.; Mayweg, A. V.; Xu, Z. H.; Qin, N.; Wong, J. C.; Zhang, Z. S.; Rong, Y. P.; Fry, D. C.; Hu, T. S. Structure-based design and synthesis of

DOI: 10.1021/acs.jmedchem.8b01402
J. Med. Chem. 2019, 62, 1291−1305

potent cyclic peptides inhibiting the YAP-TEAD protein-protein interaction. *ACS Med. Chem. Lett.* **2014**, *5*, 993−998.
(55) Kaan, H. Y. K.; Sim, A. Y. L.; Tan, S. K. J.; Verma, C.; Song, H. W. Targeting YAP/TAZ-TEAD protein-protein interactions using fragment-based and computational modeling approaches. *PLoS One* **2017**, *12*, No. e0178381.
(56) Martineau, M.; McIntosh-Smith, S.; Gaudin, W. *Evaluating OpenMP 4.0's Effectiveness as a Heterogeneous Parallel Programming Model*, 2016 IEEE 30th International Parallel and Distributed Processing Symposium Workshops; IEEE, 2016; pp 338−347.
(57) McIntosh-Smith, S.; Price, J.; Sessions, R. B.; Ibarra, A. A. High performance in silico virtual drug screening on many-core processors. *Int. J. High Perform. Comput. Appl.* **2015**, *29*, 119−134.
(58) Irwin, J. J.; Sterling, T.; Mysinger, M. M.; Bolstad, E. S.; Coleman, R. G. ZINC: A free tool to discover chemistry for biology. *J. Chem Inf. Model.* **2012**, *52*, 1757−1768.
(59) Franzen, C. A.; Chen, C. C.; Todorovic, V.; Juric, V.; Monzon, R. I.; Lau, L. F. Matrix protein CCN1 is critical for prostate carcinoma cell proliferation and TRAIL-induced apoptosis. *Mol. Cancer Res.* **2009**, *7*, 1045−1055.
(60) Alam, K. J.; Mo, J. S.; Han, S. H.; Park, W. C.; Kim, H. S.; Yun, K. J.; Chae, S. C. MicroRNA 375 regulates proliferation and migration of colon cancer cells by suppressing the CTGF-EGFR signaling pathway. *Int. J. Cancer* **2017**, *141*, 1614−1629.
(61) Noland, C. L.; Gierke, S.; Schnier, P. D.; Murray, J.; Sandoval, W. N.; Sagolla, M.; Dey, A.; Hannoush, R. N.; Fairbrother, W. J.; Cunningham, C. N. Palmitoylation of TEAD Transcription Factors Is Required for Their Stability and Function in Hippo Pathway Signaling. *Structure* **2016**, *24*, 179−186.
(62) Kaan, H. Y. K.; Chan, S. W.; Tan, S. K. J.; Guo, F. S.; Lim, C. J.; Hong, W. J.; Song, H. W. Crystal structure of TAZ-TEAD complex reveals a distinct interaction mode from that of YAP-TEAD complex. *Sci. Rep.* **2017**, *7*, No. 2035.
(63) Zhao, L.; Guan, H.; Song, C.; Wang, Y.; Liu, C.; Cai, C.; Zhu, H.; Liu, H.; Zhao, L.; Xiao, J. YAP1 is essential for osteoclastogenesis through a TEADs-dependent mechanism. *Bone* **2018**, *110*, 177−186.
(64) Joshi, S.; Davidson, G.; Le Gras, S.; Watanabe, S.; Braun, T.; Mengus, G.; Davidson, I. TEAD transcription factors are required for normal primary myoblast differentiation in vitro and muscle regeneration in vivo. *PLoS Genet.* **2017**, *13*, 31.
(65) Miesfeld, J. B.; Gestri, G.; Clark, B. S.; Flinn, M. A.; Poole, R. J.; Bader, J. R.; Besharse, J. C.; Wilson, S. W.; Link, B. A. Yap and Taz regulate retinal pigment epithelial cell fate. *Development* **2015**, *142*, 3021−3032.
(66) Berendsen, H. J. C.; Vanderspoel, D.; Vandrunen, R. Gromacs - A message-passing parallel molecular-dynamics implementation. *Comput. Phys. Commun.* **1995**, *91*, 43−56.
(67) Lindorff-Larsen, K.; Piana, S.; Palmo, K.; Maragakis, P.; Klepeis, J. L.; Dror, R. O.; Shaw, D. E. Improved side-chain torsion potentials for the Amber ff99SB protein force field. *Proteins: Struct., Funct., Bioinf.* **2010**, *78*, 1950−1958.
(68) Pettersen, E. F.; Goddard, T. D.; Huang, C. C.; Couch, G. S.; Greenblatt, D. M.; Meng, E. C.; Ferrin, T. E. UCSF chimera - A visualization system for exploratory research and analysis. *J. Comput. Chem.* **2004**, *25*, 1605−1612.

DOI: 10.1021/acs.jmedchem.8b01402
J. Med. Chem. 2019, 62, 1291−1305